Vibro-acoustic Characteristics of a Disk Brake Rotor with a Narrow Radial Slot

좁은 반경방향 슬롯을 가진 디스크 브레이크 로터의 소음방사 특성

Hyeongill Lee†
이 형 일

(Received June 4, 2009 ; Accepted August 3, 2009)

Key Words : Disk Brake(디스크 브레이크), Sound Radiation(소음방사), Slot(반경방향 슬롯), Annular Disk(환형 디스크)

ABSTRACT

Vibro-acoustic characteristics of a simplified disk-brake rotor containing a narrow radial slot are studied using a semi-analytical procedure. First, modal sound radiations for flexural and radial modes of a generic annular disk having identical key dimension and slot(with free boundaries) are defined using pre-developed analytical solutions based on the modal vibrations from finite element model. The analytical solutions are validated by fully computational methods. Second, sound radiation from a simplified brake rotor simulated using sound radiation solution of the generic disk based on the rotor eigensolutions computed using a finite element code. Predictions by the semi-analytical method matched well numerical calculations using finite element and boundary element method. Finally, sound radiation and vibration characteristics for the example rotor due to a harmonic excitation fixed to the rotor or rotating around the rotor are also obtained.

요 약

좁은 슬롯을 포함한 디스크 브레이크 로터의 소음 방사특성을 전산해석과 이론적 계산을 합성한 방법으로 검토하였다. 첫 단계로 로터와 기본 치수가 동일하고 동일한 슬롯을 보유한 후판 환형 디스크의 소음방사 특성을 유한요소해석을 구한 모달 진동 데이터를 바탕으로 기존의 해법을 이용하여 계산하고 수치해석 결과로 검증하였다. 다음으로 이 결과를 유한요소해석으로 구한 샘플 로터의 고유진동 특성에 적용, 고유진동으로 인한 소음방사를 계산한 다음 그 결과를 경계요소법을 이용하여 검증하였다. 마지막으로 이 결과를 바탕으로 로터에 고정된 조화가진 및 로터 주위를 회전하는 조화력에 의해 방사되는 소음 및 진동 특성을 검토하였다.

1. Introduction

Brake squeal is a high intensity pure tone generated by frictional interaction between rotor and pad[1~4]. The main source of squeal is the annular disk in the rotor[5,6]. Recently, introduction of asymmetries in the disk are being studied to reduce such pure tones[7]. As a representative example of such asymmetries, a narrow radial slot in the disk brake rotor is investigated here. Given

† 교신저자; 정회원, 경북대학교 기계자동차공학부
E-mail : hilee@knu.ac.kr
Tel : (054)530-1406, Fax : (054)530-1407

the complex geometries and boundaries, one has to develop detailed analyses by the finite element and boundary element methods to determine the vibro-acoustic responses of the rotor. These analyses often require significant efforts and may not lead to a basic understanding of sound radiation properties. To overcome such problems, a pre-developed semi-analytical approach has been used here. A generic disk shown in Fig. 1(a) has been studied together to simulate sound radiation from the rotor using this approach. The principal dimensions of the disk and rotor are given Table 1 along with material properties used for the structural and acoustic studies. The vibro-acoustic characteristics of the simplified disk brake rotor with a radial slot(Disk B) are simulated by those of corres-ponding generic thick annular disk with a radial slot and free boundaries at the inner and outer edges(Disk A).

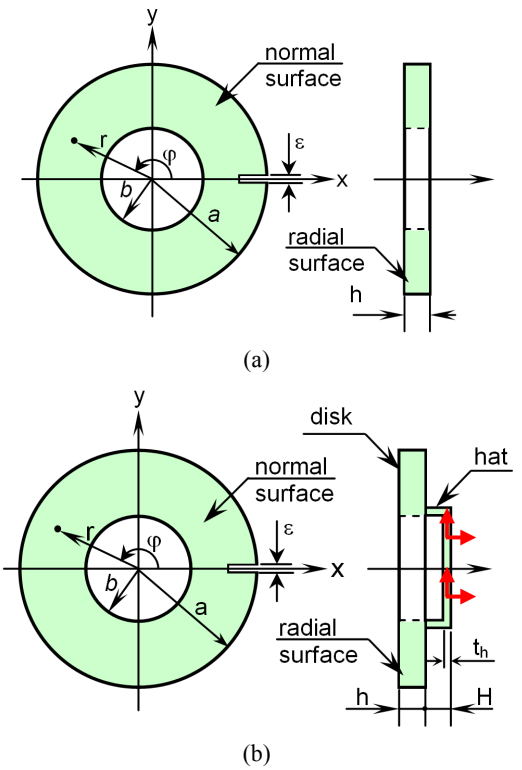

Fig. 1 Two example disks. (a) Disk A : a thick annular disk with free-free boundaries, (b) Disk B : a simplified disk-brake rotor with realistic boundaries

The generic disk(Disk A) was considered first. Structural eigensolutions are obtained using finite element method and verified with experiments. Modal sound radiation properties of the generic disk are defined by pre-developed analytical solution based on the structural eigensolutions obtained above. The results are verified numerically with a boundary element model. In this study, both in-plane and out-of-plane vibrations of the disk are considered together to completely define the vibro-acoustic properties of the disk.

Structural vibration modes of a simplified, undamped rotor with a radial slot(Disk B) are obtained by the finite-element method and compared with the vibration modes of the thick annular disk containing a radial slot(Disk A). Sound radiations from annular disk part of a brake rotor have been approximated with the radiations from the generic disk. In this study, both in-plane and out-of-plane vibrations of the disk are considered simultaneously since several modes of the rotor are combined modes which are combinations of an in-plane mode and appropriate out-of-plane mode. Semi-analytical results are validated with fully numerical results. Surface velocity and acoustic responses of the rotor to a multi-modal excitation are obtained by the modal

Table 1 Disc dimensions and material properties

Dimension or property		Disk A	Disk B
Outer radius (mm)	a	139.0	139.0
Inner radius (mm)	b	82.5	82.5
Disk thickness (mm)	h	31.5	31.5
Hat thickness (mm)	t_h	-	6.0
Hat height (mm)	H	-	24.0
Slot length (mm)	-	-	25.0
Slot width (mm)	ε	4.0	4.0
Mass density (kg/m^3)	ρ_d	7905.9	7905.9
Young's modulus (Gpa)	E	213	213
Poisson's ratio	ν	0.305	0.305

expansion technique. Also, vibro-acoustic responses of the rotor to a rotating concentrated harmonic excitation are studied.

The structural dynamic characteristics of a thick annular disks including both out-of-plane and in-plane vibration modes have been studied by many researchers[8~12]. Also, structural vibrations of thin circular or annular disks with radial slot(s) have been studied by several engineers[13~15].

In addition, sound radiation from thin or thick annular disks has been examined by a few investigators[10,12,16,17]. For instance, Lee and Singh proposed a polynomial expression for modal acoustic power radiation from a thin annular disk using the far-field sound pressure and radiation impedance approach[16]. Lee and Singh described sound radiation from in-plane or out-of-plane vibration modes of a thick annular disk[10,14,17]. The acoustic-radiation-mode concept (including the coupling effect) has been applied to an active structural-acoustic control problem as well as used to estimate radiated sound power[18~20].

Structural dynamic models have been used to explain the mechanism for brake squeal generation; theories include self-excited vibration[1] or modal coupling phenomena[2]. Recently, non-linear transient analysis[3] and complex eigenvalue approach[4] have been implemented using commercial finite-element-method codes. The underlying acoustic radiation mechanism has not been adequately examined though several attempts has been made to address this problem using measured or calculated structural vibration velocities[5,6].

The scope of the study is limited to the frequency domain analysis of a linear time invariant(LTI) system over the first few elastic modes of deformation (up to 8 kHz). Complicating effects such as fluid loading, scattering at the disk edges and rotation induced noise are not considered as they are beyond the scope of this study. Sound pressure at a receiver point(r_p) is assumed to be generated only by the vibratory motions at the disk part of the rotor and hat structure does not contribute to far-field sound pressure l.

Chief objectives of this article are as follows. (1) Examine effects of a radial slot on the structural modal datasets for the generic disk and rotor. (2) Investigate variations in modal sound radiation introduced by the narrow slot in the disc and rotor. (3) Study effects of a narrow slot on the multi-modal sound radiation from the sample rotor due to a harmonic force fixed to or rotating around the rotor.

2. Vibro-acoustic Characteristics of the Generic Disk with a Slot

2.1 Structural Characteristics

The structural characteristics of the generic disk with a radial slot are investigated with finite element models and verified with experiments[21]. According to the previous studies, radial slots incised in a thin circular or annular disk split

Table 2 Selected vibration modes of the generic disks with of without slot

Mode indices				Vibration modes		Remarks
m	n	q	l	Disk with a slot	Uniform disk	
0	2	-	c	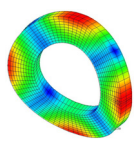	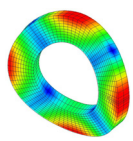	
0	2	-	s	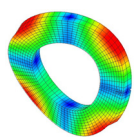		
-	-	2	c	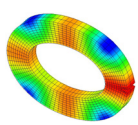	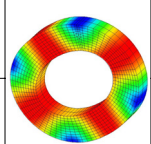	
-	-	2	s	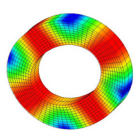		

some, but not all, repeated natural frequencies into two distinct values[13~15].

Identical phenomenon can be found in Table 2 where vibration modes of the generic disk are compared with those of corresponding uniform disk. Here, n is the order of the Bessel function representing the number of nodal diameters and m is representing the number of nodal circles. Also, q is radial mode index and l is mode split index according to the vibration mode that is c for the split mode with anti-nodal line on the slot or s for the split mode with nodal line on the slot. As one can see in the table, two split modes with same mode indices (m, n) or q are virtually same except the phase differences due to the relative location of nodal line with respect to the slot.

Eigenvalues of the generic disk are compared with those of uniform disk without any slot in Table 3. All the results are verified with the data form experimental modal analyses. All the eigenvalues of the rotor having more than one nodal lines split into two distinct values. In addition, all the eigenvalues decrease with the introduction of the radial slot but the amounts of decreases are dependent on the mode types. Also, numerical eigenvalues match well the results from experiments data for both the uniform disk and the disk with a radial slot.

Table 3 Eigenvalues for the sample disk with free-free boundaries

Mode indices				Natural frequencies			
				Disk with a slot		Uniform disk	
m	n	q	l	Numerical	Experiment	Numerical	Experiment
0	2	-	c	1477	1485	1500	1488
-	-	2	c	2612	2588	2656	2675
1	0	-	-	3479	3743	3756	3495
0	3	-	c	3867	3910	3938	3895
1	1	-	c	5311	5541	5552	5325
-	-	3	c	6523	6613	6624	6667
0	4	-	c	6838	6917	6981	6892

2.2 Modal Sound Radiation of the Generic Disk

Since thickness (h) of the disk is beyond the range of thin plate theory, radial vibration of the rotor could generate sufficient sound pressure, given a proper structural excitation[10,11]. In this study, sound radiations from the generic disk due to the in-plane modes as well as the out-of-plane modes are studied with pre-developed analytical solutions.

(1) Radiation from Out-of-plane Modes

Far-field sound pressure due to the out-of-plane modes of a thick annular disk with a radial slot can be calculated using following equations with reference to Fig. 2[5,10].

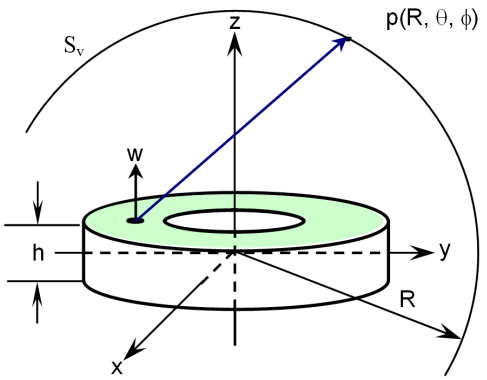

Fig. 2 Sound radiation from flexural vibration of the generic disk with free-free boundaries

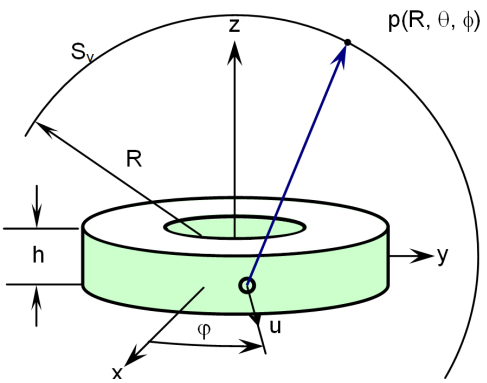

Fig. 3 Sound radiation from in-plane vibrations of the generic disk in spherical coordinate

$$
\begin{aligned}
P_{mn,l}(R,\theta,\phi) &= (1+\cos\theta)P^{s}_{mn,l}(R,\theta,\phi) \\
&\quad +(1-\cos\theta)P^{o}_{mn,l}(R,\theta,\phi) \\
P^{s}_{mn,l}(R,\theta,\phi) &= \frac{\rho_0 c_0 k_{mn,l} e^{ik_{mn,l}R}}{2R} e^{-ik_{mn,l}\frac{h}{2}\cos\theta} \times \\
&\quad \cos(n\phi+\gamma_{mn,l})(-i)^{n+1}\mathrm{B}_n\left[\dot{w}(r)\right] \\
P^{o}_{mn,l}(R,\theta,\phi) &= \frac{\rho_0 c_0 k_{mn,l} e^{ik_{mn,l}R}}{2R} e^{ik_{mn,l}\frac{h}{2}\cos\theta} \times \\
&\quad \cos(n\phi+\pi+\gamma_{mn,l})(-i)^{n+1}\mathrm{B}_n\left[\dot{w}(r)\right] \\
B_n[\dot{w}(r)] &= \int_0^{\infty} \dot{w}(r) J_n(k_r,r) r dr
\end{aligned}
\tag{1}
$$

Here, P^{s}_{mn} and P^{o}_{mn} are the sound pressures from the vibration of the two normal surfaces, ρ_0 is mass density of air, c_0 is sound speed and k is acoustic wave number k_r=$k$sinθ, and $\dot{w}(r)$ is the variation of the surface velocity on the normal surfaces in the radial direction. Further, $\gamma_{mn,l}$ is phase difference between two split modes and J_n is the Bessel function of order n.

(2) Radiation from In-plane Modes

Sound radiation due to the in-plane modes of the generic annular disk can be obtained with following equations[12,17].

$$
\begin{aligned}
P_{q,l}(R,\theta,\phi) &= P_{qI,l}(R,\theta,\phi) + P_{qO,l}(R,\theta,\phi) \\
P_{qO,l}(R,\theta,\phi) &= \frac{\rho_0 e^{ik_{q,l}R}}{\pi k_{q,l} R\sin\theta} \left|\ddot{u}_{qO}\right| h \frac{Sinc(k_{q,l}\sin\theta\, h/2)}{H_q^{1'}(k_{q,l}a\sin\theta)} \\
&\quad \times(-i)^{q+1}\cos\left(q\phi+\gamma_{q,l}\right) \\
P_{qI,l}(R,\theta,\phi) &= \frac{\rho_0 e^{ik_{q,l}R}}{\pi k_{q,l} R\sin\theta} \left|\ddot{u}_{qI}\right| h \frac{Sinc(k_{q,l}\sin\theta\, h/2)}{H_q^{2'}(k_{q,l}b\sin\theta)} \\
&\quad \times(-i)^{q+1}\cos\left(q\phi+\gamma_{q,l}\right) \\
Sinx(x) &= \frac{\sin(x)}{x}
\end{aligned}
\tag{2}
$$

Here, $P_{q,l}$ at a receiver position resulting from the q^{th} radial mode of vibration for a thick annular disk can be expressed as the sum of $P_{qO,l}$ and $P_{qI,l}$ which are sound pressure from the outer and inner radial surface respectively. $\gamma_{q,l}$ is phase difference between two split modes and H_q is the Hankel function of order q. Also, $\ddot{u}_{qO}$ and $\ddot{u}_{qI}$ are amplitudes of the acceleration on outer and inner radial surfaces, respectively. See Fig. 3 for more details.

(3) Numerical Validations

Sound pressure distributions on a sphere (S_v) surrounding the disk due to the modal vibrations of the disk are calculated using Eq. (1) and (2) defining modal sound radiations Γ_{mn} or Γ_q. Throughout this study, the radius of sphere S_v is set to be 1 m. Analytical calculations are verified with the numerical calculations using the boundary element method based on the structural data obtained in Section 2.1[22]. Experimental validations of numerical method are available in the previous studies[10,12]. The results for the selected modes are given in Table 4. As shown

Table 4 Selected modal sound radiations of the generic disk

Mode	Properties	BEM	Analytical
m =0 n = 2 q = - l = c	Pressure pattern	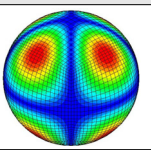	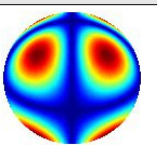
	P_{max}(dB)	199.3	196.8
m =0 n = 2 q = - l = s	Pressure pattern	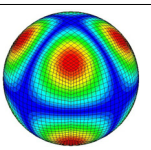	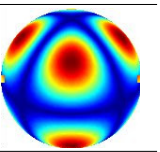
	P_{max}(dB)	199.6	196.9
m =- n = - q = 2 l = c	Pressure pattern	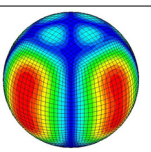	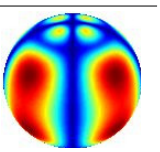
	P_{max}(dB)	206.0	205.3
m =- n = - q = 2 l = s	Pressure pattern	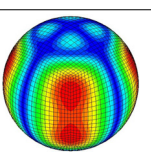	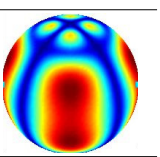
	P_{max}(dB)	208.7	205.7

in the table, modal sound radiations from two split modes with same mode indices (m, n) or q are virtually same except the phase differences due to the relative location of nodal line with respect to the slot. The maximum sound pressure (P_{max}) for $l = s$ mode is a little bit higher than that for the $l = c$ mode due to the difference in natural frequencies. In addition, the sound pressure pattern on S_v and the P_{max} from analytical calculations match well the numerical calculations for all cases. So, it can be concluded that the analytical solutions can be used to calculate sound radiations from a disk containing a slot.

3. Vibro-acoustic Characteristics of the Simplified Rotor with a Slot

3.1 Structural Characteristics

According to the previous studies, vibration modes of the disk part of the rotor can be categorized into three groups which are pure out-of-plane modes, pure in-plane modes or combined modes[5]. The combined mode caused by the coupling effect of the hat structure can be expressed as a combination of an out-of-plane mode and corresponding in-plane mode. Same phenomenon can be observed in the rotor with a radial slot. In this case, this phenomenon is accompanied with mode splits due to the radial slot. Natural frequencies and associated vibration modes are calculated using a finite element model and the results are summarized in Table 5.

As evident from the table, the q^{th} radial modes except for the $q = 0$ mode are always coupled with the $(m = 0,\ n = q)$ or $(m = 1,\ n = q)$ out-of-plane modes regardless of index l,. Also, as one can see in the table, all the modes (including out-of-plane, in-plane and combined modes) with more than one nodal line split into two distinct natural frequencies with specific frequency separations. In addition, for the given (m, n) or q, natural frequencies for the $l = s$ mode are higher than those for $l = c$ modes.

Table 5 Selected structural modes of the sample rotor

(a) Out-of-plane modes (m, n)

Mode no.	1, 2	4, 5	10, 12	13
Freq. (Hz)	1024 (l=c) 1025 (l=s)	18697 (l=c) 1874 (l=s)	4001 (l=c) 4034 (l=s)	4499
Mode shape	(0, 1) 	(0, 2) 	(0, 3) 	(1, 0) 

(b) In-plane modes (q)

Mode no.	6	20
Freq. (Hz)	2260	7653
Mode shape	Twisting 	q = 0 

(c) Combined modes (m, n and q)

Mode no.	7, 8	9, 11	18, 19
Freq. (Hz)	2884 (l=c) 2885 (l=s)	3987 (l=c) 4021 (l=s)	7118 (l=c) 7209 (l=s)
Mode shape	(0,1) + q=1 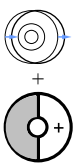	(1,2) + q=2 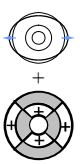	(1,3) + q=3 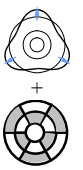

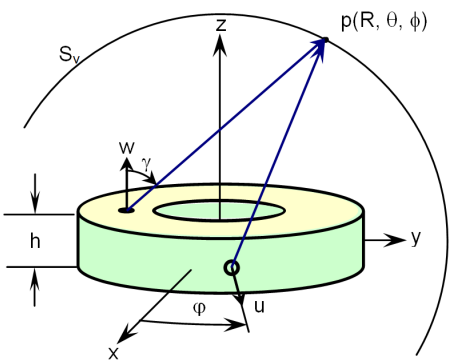

Fig. 4 Schematic representation for sound radiation from disk part of the rotor

3.2. Modal Sound Radiation from the Simplified Rotor

Sound radiations due to the modal vibration of the simplified rotor can be calculated using the analytical solutions explained in Section 2.2. As shown in Table 5, global vibration modes of the rotor are not seriously altered by the introduction of a radial slot and out-of-plane or in-plane modes can be reasonably approximated with following equations.

$$\phi_{mnqc}(r,\varphi) = W_{mn}(r)\cos n\varphi + U_q(r)\cos q\varphi$$
$$\phi_{mnqs}(r,\varphi) = W_{mn}(r)\sin n\varphi + U_q(r)\sin q\varphi \quad (3)$$

For the out-of-plane modes of the rotor where $U_q(r)$=0, sound pressures generated by normal surfaces can be directly calculated using Eq. (1). Also, in-plane modes where $W_{mn}(r)$=0 sound pressures generated by radial surfaces can be directly calculated by Eq. (2). On the other hand, the total far-field sound pressure at a given receiver position due to a combined mode can be expressed as the sum of the sound pressure from normal surfaces due to the out-of-plane vibration and that from radial surfaces due to the in-plane vibration. Note that the twisting mode is not considered in this study since it does not generate sufficient sound pressure due to its vibratory characteristics. Far-field sound pressure distributions on the S_v due to the modal vibrations of the rotor are calculated using Eq. (1) and (2) defining modal sound radiations of the rotor. In addition, based on the far-field approximation, modal acoustic powers of the rotor are calculated from modal sound pressures using following equation.

$$\Pi_{mnql} = \left\langle I_{mnql} S_V \right\rangle_s = \frac{R^2}{2\rho_0 c_0}\int_0^{2\pi}\int_0^{\pi} P_{mnql}{}^2 \sin\theta \, d\theta \, d\phi \quad (4)$$

Here, I_{mnql} are the acoustic intensity on the surface of S_V where modal sound pressure is calculated. Modal sound radiation Γ_{mnql}, maximum sound pressure P_{max} and modal acoustic powers Π_{mnql} for selected modes of the rotor are given in Table 6 along with numerical data. As shown in the table, Γ_{mnql} for out-of-plane or in-plane are quite similar to the corresponding modal sound radiation of the generic disk. Also, the results from the semi-analytical procedure match well the finite and boundary element calculations.

Table 6 Selected modal sound radiations of the brake rotor

Mode	Properties	BEM	Analytical
m =0 n = 2 q = - l = c	Pressure pattern	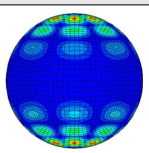	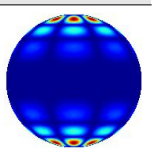
	P (dB)	216.4	216.6
	P_{max}(dB)	221.8	222.0
m = 1 n = 2 q = 2 l = c	Pressure pattern	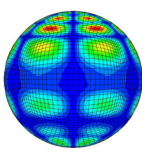	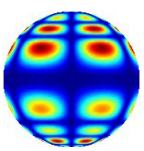
	P (dB)	210.3	210.0
	P_{max}(dB)	213.2	211.5
m = - n = - q = 0 l = -	Pressure pattern	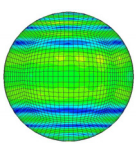	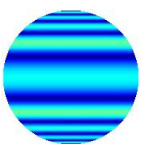
	P (dB)	217.2	216.4
	P_{max}(dB)	216.5	218.8

4. Vibro-acoustic Response to a Multi-modal Excitation

Vibro-acoustic responses of the simplified brake rotor with a radial slot for a given harmonic excitation can be obtained using modal expansion technique[5]. If the disk is excited by a multi-modal harmonic force at an arbitrary location $\boldsymbol{r}_f = (r_f, \varphi_f)$ and circular frequency ω, several modes, including both split and repeated modes, are simultaneously excited. Based on the modal expansion technique, velocity distribution (v) on the rotor surfaces can

be expressed in terms of modal velocity vectors as shown in the following equations.

$$\{v(\omega)\} = \{\eta(\omega)\}^T \{\Phi^V\}$$
$$\{\eta(\omega)\} = \{\eta_1, \eta_2, \eta_3, \cdots, \eta_j\} \quad (5)$$

In Eq. (5), ϕ^v is the modal velocity vector of the disk expressed as the modal displacement vector multiplied by the corresponding natural frequency (in rad/s) and η_l is the associated modal participation factor that can be expressed as follows assuming unit harmonic force.

$$\eta_l(\omega) = \frac{\phi_l(r_f, \varphi_f)}{\omega_l^2 \left[1 - \omega^2/\omega_l^2 + i2\varsigma_l(\omega/\omega_l)\right]} \quad (6)$$

Here, ω_1 and ζ_1 are the natural frequency and modal damping ratio of mode 1, respectively.

Earlier, Lee and Singh expressed the far-field sound pressure from thin or thick annular disks due to a multi-modal excitation using the structural modal participation factors and modal sound radiations[13,19]. Applying the same procedure to the rotor acoustic problem, the far-field pressure on S_v surrounding the rotor given the surface velocity of Eq. (5) can be expressed as :

$$P(\omega) = \{\eta(\omega)\}^T \{\Gamma\};$$
$$\{\Gamma\} = \{\Gamma_1, \Gamma_2, \Gamma_3, \cdots, \Gamma_l\}. \quad (7)$$

Here, Γ_l is the modal sound radiation for mode 1.

Acoustic power $\Pi(\omega)$ of the rotor due to an arbitrary harmonic excitation $f(t)$ can also be obtained from the far-field sound pressures on S_v as :

$$\Pi(\omega) = \frac{1}{2}\int_0^{2\pi}\int_0^{\pi} \frac{P^H(\omega)P(\omega)}{\rho_0 c_0} R^2 \sin\theta \, d\theta \, d\phi \quad (8)$$

4.1. Responses to a Harmonic Excitation Fixed to the Rotor

The modal participation factor η in Eq. (6) can be expressed as follows considering vibration shapes of two modes given in Eq. (3) and the assumptions in Section 1.

$$\eta_{mnql}(\omega) = \frac{\phi_{mnql}(r_f, \varphi_f)}{\omega_{mnql}^2 \left[1 - \omega^2/\omega_{mnql}^2 + i2\varsigma_{mnql}(\omega/\omega_{mnql})\right]} \quad (9)$$

Consequently, total surface velocity and sound pressure distributions due to a unit harmonic excitation in the normal or radial directions at $\boldsymbol{r}_f$ with circular frequency ω can be expressed as follows.

$$v(\omega) \cong \sum\sum\sum \left(\frac{\phi_{mnqc}\cos n\varphi_f}{\omega_{mnqc}^2 - \omega^2 + i2\varsigma_{mnqc}\omega\omega_{mnqc}} + \frac{\phi_{mnqs}\sin n\varphi_f}{\omega_{mnqs}^2 - \omega^2 + i2\varsigma_{mnqs}\omega\omega_{mnqs}} \right) \{W_{mn}(r_f) + U_q(r_f)\} \quad (10)$$

$$p(\omega) \cong \sum\sum\sum \left(\frac{\Gamma_{mnqc}\cos n\varphi_f}{\omega_{mnqc}^2 - \omega^2 + i2\varsigma_{mnqc}\omega\omega_{mnqc}} + \frac{\Gamma_{mnqs}\sin n\varphi_f}{\omega_{mnqs}^2 - \omega^2 + i2\varsigma_{mnqs}\omega\omega_{mnqs}} \right) \{W_{mn}(r_f) + U_q(r_f)\} \quad (11)$$

As one can imagine from Eq. (10) and (11), surface velocity and sound radiation for the given excitation are significantly affected by the location of excitation. For instance, ϕ_{mnqc} or Γ_{mnqc} does not contribute to total vibration and sound radiation when $\varphi_f = 0$ or $\varphi_f = \pi/2$ for the example case given in Fig. 1 and Table 1.

$p/f(\omega)$ at R = 1.0, $\theta = \pi/4$ and $\phi = \pi/2$ for a unit harmonic excitations in normal direction at r = 0.139, $\varphi = -\pi/8$ and $r = 0.139$, $\varphi = \pi$ have been calculated using Eq. (11). The results are compared with numerical calculations in Fig. 5. As one can see in the figure, $p/f(\omega)$ is significantly affected by the location of excitation. Also, analytical calculation match well the numerical results for all cases.

$\Pi/f(\omega)$ due to the harmonic excitation given above have also been calculated using Eq. (8). The results are compared with numerical calculations in Fig. 6. As in the case of $p/f(\omega)$, $\Pi/f(\omega)$ is affected significantly by the location of excitation. In

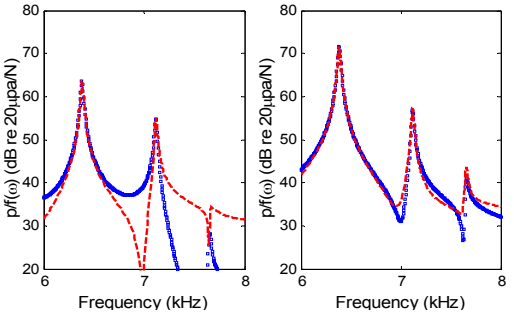

Fig. 5 $p/f(\omega)$ at $r_p = (1,\ \pi/4,\ \pi/2)$ for the selected r_{fs}. (a) $r_f = (0.139,\ -\pi/12)$ (b) $r_f = (0.139,\ \pi)$. Key : ▫ ▫ ▫, Analytical ; - - -, Numerical

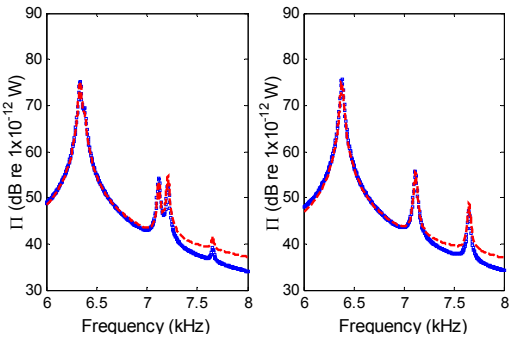

Fig. 6 $\Pi/f(\omega)$ for a harmonic force at the selected r_f. (a) $r_f = (0.139,\ -\pi/12)$ (b) $r_f = (0.139,\ \pi)$. Key : ▫ ▫ ▫, Analytical ; - - -, Numerical

addition, analytical calculation match well the numerical results for all cases especially at the vicinities of natural frequencies.

4.2. Response to a Moving Load

If the natural frequencies of two split modes of the rotor are sufficiently separated from each other with respect to damping factors, the resonant modes are fixed in the disk fixed coordinate system[15]. But, if the natural frequency separation is small relative to the damping, two split modes act like a pair of repeated modes. The surface velocity distribution and far-field sound pressure due to a rotating harmonic excitation in normal direction can be expressed as following equations

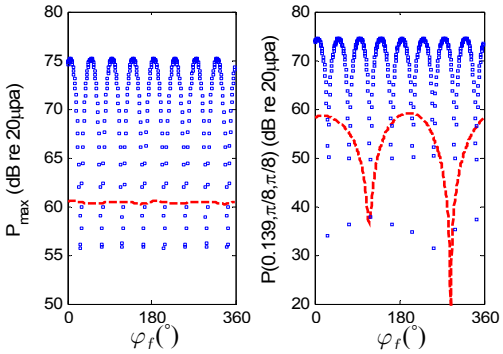

Fig. 7 Sound pressure due to a rotating harmonic excitation (a) p_{max} (b) p at $r_p = (0.139,\ \pi/8,\ \pi/8)$. Key : ▫ ▫ ▫, $f = 6337$ Hz ; - - -, $f = 1024$ Hz

assuming that angular velocity of the moving force is slow ($\omega_r << \omega_{mnql}$) and damping is light.

$$v(r,\varphi,t) \cong \sum\sum\sum \left\{ \frac{\phi^V_{mnqc}(r,\varphi)\cos n(\omega_r t)}{\omega^2_{mnqc} - \omega^2 + i2\varsigma_{mnqc}\omega\omega_{mnqc}} + \frac{\phi^V_{mnqs}(r,\varphi)\sin n(\omega_r t)}{\omega^2_{mnqs} - \omega^2 + i2\varsigma_{mnqs}\omega\omega_{mnqs}} \right\} W_{mn}(r_0) e^{i2\pi ft} \tag{12}$$

$$p(R,\theta,\phi,t) \cong \sum\sum\sum \left\{ \frac{\Gamma_{mnqc}(R,\theta,\phi)\cos n(\omega_r t)}{\omega^2_{mnqc} - \omega^2 + i2\varsigma_{mnqc}\omega\omega_{mnqc}} + \frac{\Gamma_{mnqs}(R,\theta,\phi)\sin n(\omega_r t)}{\omega^2_{mnqs} - \omega^2 + i2\varsigma_{mnqs}\omega\omega_{mnqs}} \right\} W_{mn}(r_0) e^{i2\pi ft} \tag{13}$$

Here, r_0 and ω_r are radial position and rotating speed of the rotating harmonic force, respectively and f is excitation frequency.

The maximum sound pressure on S_v and P at a specific receiver position due to a rotating harmonic force in the normal direction with a frequency that coincides with one of the natural frequencies of the rotor are obtained using Eq. (13). The result is explained in Fig. 7 where it is clear that the amplitudes of sound pressures for the rotating force with frequency of 6337 Hz have sinusoidal variations within one revolution of force. But, the maximum sound pressure for the

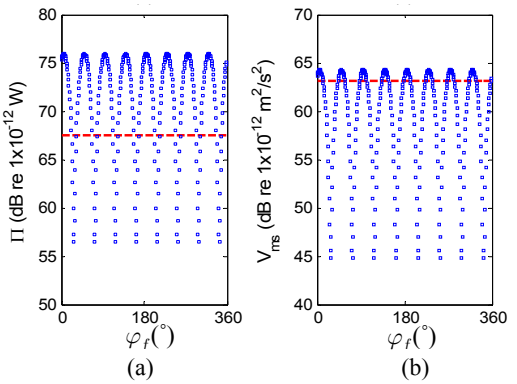

Fig. 8 Acoustic power and surface velocity due to a rotating harmonic excitation (a) Π (b) V_{ms}. Key : ▫ ▫ ▫, f = 6337 Hz ; - - -, f = 1024 Hz

force of frequency 1024 Hz is relatively flat with very small variation. In addition, acoustic power and mean square velocity on the surfaces of the disk due to the same rotating force are also calculated using Eq. (12) and (13). The results are explained in Fig. 8. As shown in the figure, powers and velocities for the force of 6337 Hz have 1024 Hz are almost sinusoidal variation and those for the force of constant during one revolution of the force.

Finally, it can be inferred that the resonant modes of a uniform rotor are fixed in the force fixed coordinate system and surface velocity and sound pressure distributions rotate with the applied force. Consequently, acoustic powers and mean square velocity are constant during one revolution of the force regardless of the location of the force.

3. Conclusion

Vibro-acoustic characteristics of a simplified rotor with a narrow radial slot have been investigated using a semi-analytical procedure combining numerical calculations for structural properties and analytical solutions for acoustic radiations. Annular disk part of the rotor has been modeled as a thick annular disk with same geometric configuration and the identical radial slot. Numerical validation shows that sound radiation of the rotor can be accurately simulated with those of the generic disk.

Sound radiations due to a multi-modal harmonic force fixed to the rotor can be accurately calculated using the modal expansion technique based on the modal sound radiations above. The results match well the numerical calculations using the boundary element method. Finally, vibro-acoustic responses due to a rotating harmonic force of one of the split natural frequencies have also been studied. Maximum sound pressure, acoustic power and mean square velocity have sinusoidal variations within one revolution when frequency separation is big enough with respect to the modal damping. On the contrary, when the separation is small relative to the modal damping, acoustic properties are almost constant regardless of excitation location as in the case of uniform rotor.

Important extensions of this study include the following research problems. (1) Investigate the effects of the radial slot(s) on the modal coupling between a brake rotor and neighboring components. (2) Investigate the effects of the radial slot(s) on the stability of total brake system modes.

Acknowledgement

This work was supported by the Kyungpook National University Research Grant, 2009.

References

(1) Murakami, H., Tsunada, N. and Kitamura, T., 1984, “A Study Concerned with a Mechanism of Disc-brake Squeal,” SAE Technical Paper 841233.

(2) Flint, J. and HultÈn, J., 2002, “Lining-deformation-induced Modal Coupling as Squeal Generator in a Distributed Parameter Disc Brake Model,” Journal of Sound and Vibration, Vol. 254, No. 1, pp. 1~21.

(3) Hu, Y. K. and Nagy, L. I., 1997, "Brake Squeal Analysis by Using Nonlinear Transient Finite Element Method," SAE Technical Paper 971510.

(4) Kung, S. W., Dunlap, K. B. and Ballinger, R. S., 2000, "Complex Eigenvalue Analysis for Reducing Low Frequency Squeal," SAE Technical Paper 2000-01-0444.

(5) Lee, H. and Singh, R., 2004, "Determination of Sound Radiation from a Simplified Disk Brake Rotor Using a Semi-analytical Method," Noise Control Engineering Journal, Vol. 52, No. 5, pp. 457~472.

(6) McDaniel, J. G., Moore, J., Chen, S. and Clarke, C. L., 1999, "Acoustic Radiation Models of Brake Systems from Stationary LDV Measurement," Proc. IMEC 99, Nashville,Tennessee.

(7) Fieldhouse, J. D., Steel, W. P., Talbot, C. J. and Siddiqui, M. A., 2004, "Rotor Asymmetry Used to Reduce Disc Brake Noise," SAE Technical Papers 2004-01-2797.

(8) Mindlin, R. D. and Deresiewicz, H., 1954, "Thickness-shear and Flexural Vibration of a Circular Disk" ASME Journal of Applied Physics Vol. 25, No. 10, pp. 1329~1332.

(9) Mcgee, O. G., Huang, C. S. and Leissa, A. W., 1995, "Comprehensive Exact Solutions for Free Vibrations of Thick Annular Sectorial Plates with Simply Supported Radial Edges," International Journal of Mechanical Science, Vol. 37, No. 5, pp. 537~566.

(10) Lee, H. and Singh, R., 2005, "Acoustic Radiation from Out-of-plane Modes of an Annular Disk Using Thin and Thick Plate Theories," Journal of Sound and Vibration, Vol. 282, No. 1-2, pp. 313~339.

(11) Irie, T., Yamada, G. and Muramoto, Y., 1984, "Natural Frequencies of In-plane Vibration of Annular Plates," Journal of Sound Vibration, Vol. 97, No. 1, pp. 171~175.

(12) Lee, H., 2005, "Acoustic Radiation from Radial Vibration Modes of a Thick Annular Disk," Transactions of the Korean Society for Noise and Vibration Engineering, Vol. 9, No. 6, pp. 1210~1217.

(13) Yu, R. C. and Mote, C. D. JR., 1987, "Vibration and Parametric Excitation in Asymmetric Circular Plates under Moving Load," Journal of Sound and Vibration, Vol. 119, No.3, pp. 409~427.

(14) Shen, I. Y. and Mote, C. D. JR., 1992, "Dynamic Analysis of Finite Linear Elastic Solids Containing Small Elastic Imperfections: Theory with Application to Asymmetric Circular Plates," Journal of Sound and Vibration, Vol. 155, No. 3, pp. 443~465.

(15) Honda, Y., Matsuhisa, H. and Sato, S., 1985, "Modal Response of a Disk to a Moving Concentrated Harmonic Force," Journal of Sound and Vibration, Vol. 102, No. 4, pp. 457~472.

(16) Lee, M. R. and Singh, R., 1994, "Analytical Formulations for Annular Disk Sound Radiation Using Structural Modes," Journal of Acoustical Society of America, Vol. 95, No. 6, pp. 3311~3323.

(17) Lee, H. and Singh, R., 2005, "Comparison of Two Analytical Methods Used to Calculate Sound Radiation from Radial Vibration Modes of A Thick Annular Disk," Journal of Sound and Vibration, Vol. 285, No. 4-5, pp. 1210~1216.

(18) Gibbs, G. P., Clark, R. L., Cox, D. E. and Vipperman, J. S., 2000, "Radiation Modal Expansion: Application to Active Structural Acoustic Control," Journal of Acoustical Society of America, Vol. 107, No. 1, pp. 332~339.

(19) Bai, M. R. and Tsao, M., 2002, "Estimation of Sound Power of Baffled Planar Sources Using Radiation Matrices," Journal of Acoustical Society of America, Vol. 112, No. 3, pp. 876~883.

(20) Lee, H. and Singh, R., 2005, "Self and Mutual Radiation from Flexural and Radial Modes of a Thick Annular Disk," Journal of Sound and Vibration, Vol. 286, No. 4-5, pp. 1032~1040.

(21) I-DEAS User's manual Version 11 (UGS Corporation, USA, 2006).

(22) SYSNOISE User's Manual Version 5.6 (Numerical Integration Technologies N.V., Belgium, 2005).